Adsorptive Removal of Malachite Green from Synthetic Wastewater Using Bamboo Activated Carbon

Teewara Teerasukyodying[1], Nagone Luangphaiboonsri[2], Weerawat Clowutimon[1,3,*], and Pornsawan Assawasaengrat[4]

[1] Department of English Program, Samsenwittayalai School, Bangkok, 10400, Thailand
[2] Chulalongkorn University Demonstration Secondary School, Bangkok, 10330, Thailand
[3] Department of English Program, Satriwittaya School, Bangkok, 10200, Thailand
[4] Department of Chemical Engineering, School of Engineering, King Mongkut's Institute of Technology Ladkrabang, Bangkok, 10520, Thailand
Email: ss53321@samsenwit.ac.th (T.T.); s65049@satitm.chula.ac.th (N.L.); t.weerawat@samsenwit.ac.th (W.C.); Pornsawan_as@kmitl.ac.th (P.A.)
*Corresponding author
Manuscript received January 1, 2026; accepted February 27, 2026; published April 30, 2026

***Abstract*—The adsorptive removal of Malachite Green (MG) using Bamboo-derived Activated Carbon (BAC) was investigated. Bamboo biochar was chemically activated with KOH and carbonized at 700 °C for 3 h to produce BAC. The prepared material was characterized using Scanning Electron Microscope (SEM), Carbon, Hydrogen, Nitrogen, Sulfur (CHNS), X-Ray Diffraction (XRD), Fourier Transform Infrared Spectroscopy (FT-IR), and Brunauer Emmett Teller (BET) analyses. Batch adsorption experiments were conducted using an adsorbent dosage of 0.25 g in 50 mL of MG solution to evaluate the effects of initial dye concentration and contact time on adsorption performance. The characterization results confirmed that BAC possesses favorable surface and textural properties for MG adsorption. Adsorption equilibrium was achieved within 60 min, and the equilibrium data were better described by the Langmuir isotherm model than by the Freundlich model, indicating that MG adsorption occurs predominantly via a favorable monolayer physisorption mechanism.**

***Keywords*—adsorption, activated carbon, bamboo, malachite green, wastewater**

I. Introduction

Water pollution is one of the most serious global environmental issues. This pollution mainly arises from rapid urbanization and industrialization. A major source of water contamination is the direct discharge of wastewater containing synthetic dyes. Among these dyes, Malachite Green (MG), a cationic triphenylmethane dye with the chemical formula $C_{23}H_{25}ClN_2$, is widely used in the textile, pigment, paper, pulp, wool, and silk industries. Due to its complex aromatic structure, MG is highly resistant to degradation in aquatic environments. The presence of MG in water poses significant toxicity to aquatic organisms and can also endanger human health, causing teratogenicity, carcinogenicity, and even paralysis through the consumption of contaminated water [1]. Therefore, a pretreatment process is essential before wastewater containing MG is discharged into the environment.

Among various treatment methods, adsorption is considered one of the most effective approaches because of its simple design and operation, low energy consumption, cost-effectiveness, and ease of adsorbent regeneration [2–3]. Owing to these advantages, many recent studies on wastewater pretreatment have focused on adsorption techniques. Activated Carbon (AC) is one of the most commonly used adsorbents worldwide. It is typically produced from carbon-rich precursors such as coconut shells, bamboo, and other lignocellulosic biomass materials. The preparation process of AC involves two key stages: pyrolysis and activation. During pyrolysis, volatile components and most of the hydrogen, oxygen, and nitrogen are removed, thereby increasing the fixed carbon content. The subsequent activation process enhances the surface area and pore volume of the resulting charcoal. Activation can be achieved through physical, chemical, or combined methods. Compared to physical activation, chemical activation generally produces higher surface areas and larger total pore volumes [4–6], while also requiring lower activation temperatures. Among the various chemical agents, potassium hydroxide (KOH) is widely used because it produces well-developed pore structures and high surface areas [4–5, 7–8]. During activation, the reaction between potassium species and the carbon framework generates metallic potassium and gaseous products that expand the lattice and create micro- and mesopores. The main reactions can be represented as follows [7]:

$$6KOH + 2C \rightarrow 2K + 3H_2 + 2K_2CO_3 \quad (1)$$

$$K_2CO_3 \rightarrow K_2O + CO_2 \quad (2)$$

$$CO_2 + C \rightarrow 2CO \quad (3)$$

$$2C + K_2CO_3 \rightarrow 2K + 3CO \quad (4)$$

$$K_2O + C \rightarrow 2K + CO \quad (5)$$

These reactions promote the intercalation of metallic potassium into the carbon matrix and the evolution of gases (H_2, CO_2, CO), leading to lattice expansion and pore formation. Upon washing to remove potassium residues, a highly porous carbon structure remains, which is favorable for adsorption applications.

According to previous studies, bamboo-derived activated carbon has been used for the removal of various pollutants such as heavy metals [9, 10], rhodamine B [11], methylene blue [12], and methyl orange [13]. However, reports on the use of Bamboo Activated Carbon (BAC) for the removal of MG from wastewater remain limited.

In this study, the adsorptive removal of MG from synthetic wastewater using BAC prepared via KOH activation was investigated. The effects of key parameters, including contact

time and initial dye concentration, were evaluated in a batch adsorption system. The findings of this study aim to highlight bamboo-derived activated carbon as an environmentally friendly and sustainable adsorbent for wastewater treatment applications.

II. Materials and Methods

A. Materials

Bamboo used in this study was obtained from a local forest farm in Nakorn Ratchasima Province, Thailand. All chemicals used were analytical grade. Hydrochloric acid (HCl) and KOH were supplied by KemAus (Australia) and MG was purchased from Loba Chem (India).

B. Preparation of Activated Carbon from Bamboo

Bamboo was initially cut into small pieces, washed with deionized water to remove surface dust, and dried in an oven (OF-01E, JEIO TECH) at 105 °C overnight. A fixed amount of the dried bamboo (approximately 10 g) was placed in a furnace (CWF 1100, Carbolite) and carbonized at 400 °C for 3 h without gas purging. The resulting carbonized bamboo was then cooled to room temperature and mixed with a KOH solution at a mass ratio of carbonized bamboo to KOH of 1:4. The mixture was stirred for 30 min and subsequently aged for 24 h. After aging, the sample was separated by filtration and dried in an oven at 105 °C overnight. The dried material was then activated in the furnace at 700 °C for 3 h. After activation, the AC was washed with 0.1 M HCl, followed by deionized water until a neutral pH was reached. Finally, the sample was dried in the oven and characterized using scanning electron microscopy (SEM; JSM-IT300, JEOL), elemental analyzer (Flashsmart, Thermo), X-ray diffraction (XRD; D8 Discover, Bruker), Fourier-transform Infrared spectroscopy (FT-IR; INVENIO S, Bruker), and Brunauer-Emmett-Teller analysis (BET; Autosorb Automated gas sorption analysis, Quantachrome Instruments).

C. Adsorption Experiments

Adsorption experiments were conducted in batch mode by adding 0.25 g of BAC to 50 mL of MG solution with initial concentrations ranging from 10 to 500 mg/L. The solution was stirred using a magnetic stirrer (SP-200T, Miulab) at a constant speed of 350 rpm and the temperature was maintained at 30 °C. Samples were withdrawn at predetermined time intervals ranging from 5 to 180 min. The adsorbent was separated using a nylon syringe filter (0.45 µm, Anpell). The residual concentration of MG in the filtrate was determined using a UV-Visible spectrophotometer (T60 V, PG Instruments) at a wavelength of 617 nm. The amount of MG adsorbed at time t (q_t) was calculated using Eq. (6).

$$q_t = \frac{(C_0 - C_t)V}{W} \quad (6)$$

where C_0 and C_t are the initial concentration and the concentration of MG at time t (mg/L), respectively, V is the volume of solution (mL) and W is weight of the adsorbent (g).

III. Results and Discussion

A. Characterization of BAC

Scanning Electron Microscope (SEM) analysis was performed to examine the surface morphology of bamboo charcoal (before activation) and BAC (after activation). The results are shown in Fig. 1. As seen in Fig. 1(a), the surface of the bamboo charcoal appears relatively smooth and compact. After activation, the material becomes highly porous with numerous cavities and irregular channels (Fig. 1(b)), confirming the successful transformation of bamboo charcoal into BAC. The formation of these pores can be attributed to the KOH activation process, during which reactions between potassium species and the carbon framework generate gaseous products and promote lattice expansion, as discussed earlier in the introduction.

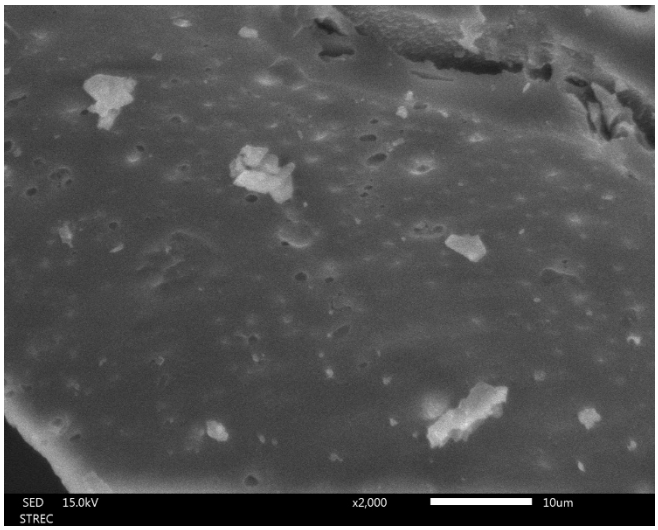

(a)

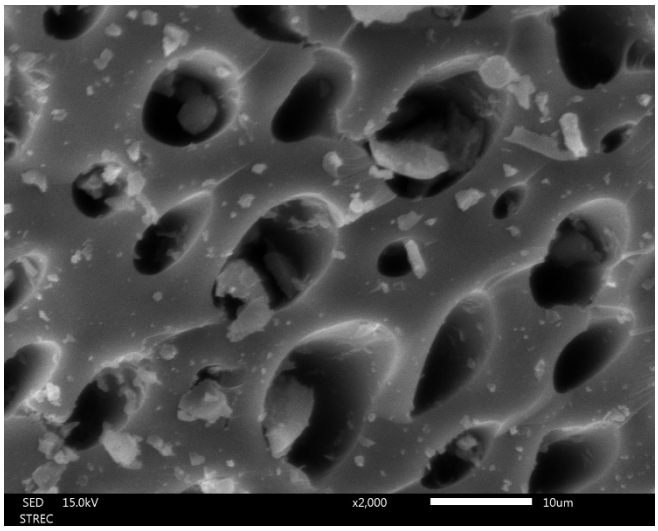

(b)

Fig. 1. SEM images of (a) bamboo charcoal before activation and (b) BAC after KOH activation at 700 °C for 3 h.

Elemental (CHNS) analysis was performed to determine the composition of carbon, hydrogen, nitrogen, and sulfur in the BAC. The results are summarized in Table 1. The carbon content of the BAC is approximately 79%, indicating that carbon is the predominant element in the material. The relatively low hydrogen and nitrogen contents suggest the removal of most organic and volatile components during carbonization and activation. These results are consistent with those reported for activated carbon prepared from other lignocellulosic materials [14–16].

Table 1. Element composition of BAC

Element	% wt.
C	79.15
H	1.53
N	0.36
S	-
O (by difference)	18.96

XRD analysis was performed to examine the crystal structure and degree of crystallinity of the BAC. The XRD pattern is shown in Fig. 2. The diffraction pattern exhibits a broad peak in the range of 2θ = 15°–25° and the absence of any sharp diffraction peaks, indicating that the material possesses a predominantly amorphous structure. Such an amorphous nature is a characteristic of AC and is considered favorable for adsorption applications due to the presence of numerous disordered sites that can enhance adsorptive interactions.

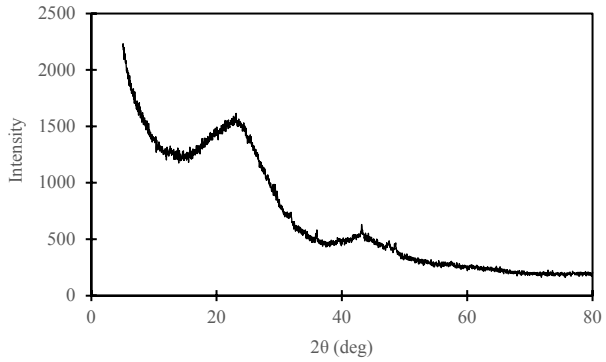

Fig. 2. XRD pattern of BAC.

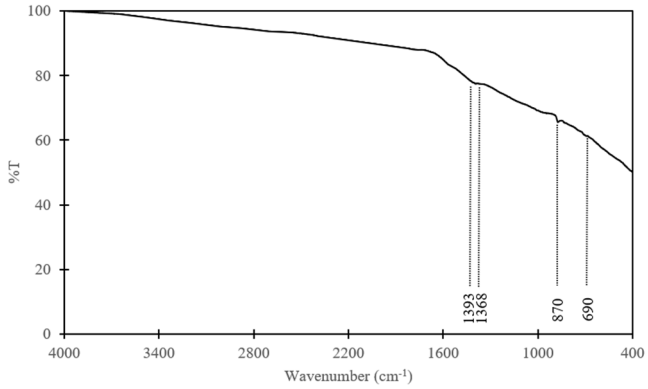

Fig. 3. FT-IR spectrum of BAC.

FT-IR analysis was conducted to identify the surface functional groups of the BAC. The FT-IR spectrum (Fig. 3) shows weak and broad absorption bands at approximately 1390–1370, 870, and 690 cm^{-1}. The band at 1390–1370 cm^{-1} can be attributed to the deformation vibration of aliphatic $–CH_3$ groups or, alternatively, to the symmetric stretching of minor carboxylate ($–COO^-$) species. The bands at around 870 cm^{-1} and 690 cm^{-1} correspond to out-of-plane aromatic C–H bending modes [17], indicating the presence of residual aromatic fragments and condensed aromatic domains within the carbon matrix. The absence of strong absorption bands corresponding to hydroxyl (–OH), carbonyl (C=O), and carboxyl (–COOH) groups suggests that most oxygenated surface functionalities were decomposed during high-temperature activation [18]. This reduction in surface oxygen is consistent with the carbonization process and supports the formation of a predominantly amorphous carbon framework, as confirmed by the XRD results. Nevertheless, Carbon, Hydrogen, Nitrogen, Sulfur (CHNS) analysis indicates that the material still contains approximately 19 wt.% oxygen, implying the presence of a small amount of residual oxygen-containing groups such as –OH, C=O, and –COOH, although they were weakly detected by FT-IR.

BET analysis was employed to determine the specific surface area, total pore volume, and average pore diameter of the prepared BAC, and the results are summarized in Table 2. The BAC exhibited an average pore diameter of 1.19 nm, indicating a predominantly microporous structure (<2 nm), which is comparable to BAC prepared using other chemical activating agents, particularly potassium carbonate (K_2CO_3) [11, 19–21]. This pore size is larger than the molecular dimension of MG (≈ 0.82 nm) [22], suggesting that the pore structure of the BAC is suitable for MG adsorption via a micropore-filling mechanism. The BET surface area and total pore volume of the BAC were 395.82 m^2/g and 0.22 cm^3/g, respectively. These values are relatively lower than those reported in previous studies for BAC prepared with KOH, as well as with other chemical activating agents [11, 12, 19–21]. Such differences in textural properties can be attributed to variations in activation parameters, including activation temperature, activation duration, and activating agent-to-char ratio, as higher temperatures and increased chemical impregnation ratios have been shown to promote more extensive pore development and significantly higher surface areas [23, 24]. Nevertheless, the activation conditions employed in this study produced a well-developed microporous AC structure that is adequate for effective MG adsorption, while further optimization of activation parameters could enhance the surface area and pore volume.

Overall, the characterization results confirm that the prepared BAC possesses a carbon-rich, porous, and amorphous structure with a moderately large surface area and limited but active oxygen functionalities, making it favorable for dye adsorption.

Table 2. BET surface area, pore volume, and pore diameter of BAC

Material	Total surface area (m^2/g)	Total pore volume (cm^3/g)	Average pore diameter (nm)
Bamboo activated carbon	395.82	0.22	1.19

B. Adsorption Experiment Results

Preliminary batch adsorption experiments were conducted to determine the equilibrium adsorption time at different initial concentrations of MG. The results, as shown in Fig. 4, indicate that MG adsorption increases rapidly during the initial stage of the process. For an initial concentration of 20 ppm, rapid adsorption occurs within the first 20 min, whereas for initial concentrations of 50 and 100 ppm, this rapid uptake extends to approximately 60 min. After this initial period, the adsorption rate gradually decreases until equilibrium is reached at around 120 min for all concentrations. The fast uptake at the early stage is associated with the large number of available adsorption sites on the surface of the activated carbon. As adsorption proceeds, these sites are progressively occupied, leading to a decrease in the adsorption rate and the eventual attainment of equilibrium. Moreover, higher initial

MG concentrations result in faster adsorption rates due to an increased concentration gradient between the bulk solution and the adsorbent surface, which enhances the mass-transfer driving force. To ensure that adsorption equilibrium was fully achieved in subsequent adsorption isotherm studies, a contact time of 180 min was selected for all experiments.

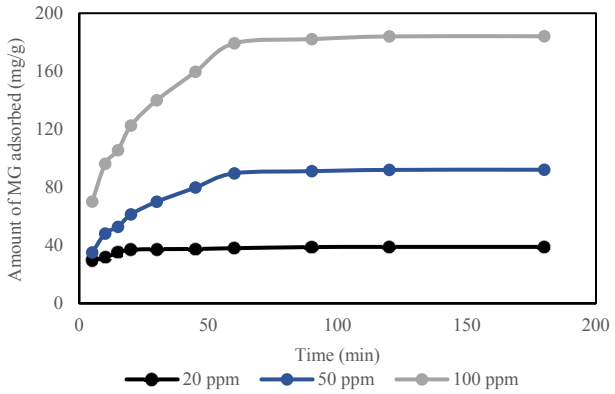

Fig. 4. Adsorption kinetics of MG onto BAC at different initial concentrations (20, 50, and 100 mg/L) with an adsorbent dosage of 0.25 g.

The adsorption isotherm study was conducted in a batch system by varying the initial concentration of MG from 10 to 500 mg/L. The equilibrium adsorption behavior is presented in Fig. 5. As shown, the equilibrium adsorption capacity (q_e, mg/g) increased rapidly and almost linearly at low equilibrium concentrations (C_e, mg/L), particularly below 20 mg/L. This behavior can be attributed to the abundant availability of active adsorption sites on the adsorbent surface and the strong concentration gradient between the bulk solution and the adsorbent, which provides a high driving force for mass transfer. As the equilibrium concentration increased further, the increase in q_e became more gradual and eventually approached a plateau, indicating that the available adsorption sites were progressively occupied and that the maximum adsorption capacity (q_{max}) had been reached. This adsorption trend suggests a surface-saturation-controlled process with a finite number of active sites on the BAC.

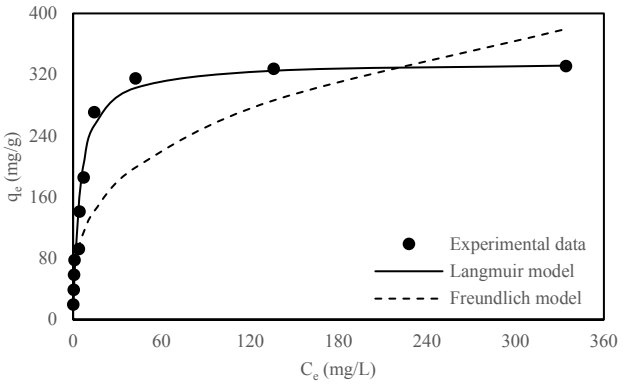

Fig. 5. Adsorption isotherm of MG onto BAC, obtained at various initial concentrations (10–500 mg/L) with an adsorbent dosage of 0.25 g and a contact time of 180 min, fitted with Langmuir and Freundlich models.

The adsorption equilibrium behavior was analyzed using the Langmuir and Freundlich isotherm models, as expressed in Eqs. (7) and (8), respectively:

$$q_e = \frac{q_{max} K_L C_e}{1 + K_L C_e} \quad (7)$$

$$q_e = K_F C_e^{\frac{1}{n}} \quad (8)$$

where K_L (L/mg) is the Langmuir constant related to adsorption affinity, and K_F ($(mg/g)(L/mg)^{\frac{1}{n}}$) and n are the Freundlich constants associated with adsorption capacity and adsorption intensity, respectively.

The isotherm parameters obtained from the experimental data, together with the corresponding correlation coefficients (R^2), are summarized in Table 3. The Langmuir model exhibited a significantly higher correlation coefficient (R^2 = 0.9995) than the Freundlich model (R^2 = 0.8560), indicating that the Langmuir model provides a better description of the adsorption equilibrium, particularly at higher equilibrium concentrations, as shown in Fig. 5. This result suggests that adsorption predominantly occurs through monolayer coverage on an energetically homogeneous surface, where each adsorption site accommodates a single adsorbate molecule.

Table 3. Langmuir and Freundlich model parameters

Model	Parameter	Value
Langmuir	q_{max} (mg/g)	336.50
	K_L (L/mg)	0.212
	R^2	0.9995
Freundlich	K_F $\left((mg/g)(L/mg)^{\frac{1}{n}}\right)$	62.6
	n	3.09
	R^2	0.8560

The favorability of the adsorption process was further evaluated using the Langmuir separation factor (R_L), calculated according to Eq. (9):

$$R_L = \frac{1}{1 + K_L C_0} \quad (9)$$

The obtained R_L values ranged from 9.34×10^{-3} to 3.21×10^{-1}, falling within the range $0 < R_L < 1$, confirming favorable adsorption behavior. In addition, the Freundlich constant n was greater than 1 ($n = 3.09$), further supporting that the adsorption process is favorable and mainly governed by physisorption [25–26].

The adsorption mechanism can be attributed to the combined effects of surface chemistry and pore accessibility of the BAC. Residual oxygen-containing functional groups, as indicated by CHNS and FT-IR analyses, may contribute to adsorption through electrostatic interactions and hydrogen bonding. Since MG is a cationic dye, electrostatic attraction between the positively charged dye molecules and negatively charged surface sites plays an important role. In addition, π–π interactions between the aromatic rings of MG and the graphitic domains of the carbon framework may further enhance adsorption. The favorable pore structure identified by BET analysis enables effective diffusion of dye molecules into the internal adsorption sites, supporting the observed high adsorption capacity and rapid attainment of equilibrium [27].

A comparative evaluation of q_{max} of the prepared BAC with other reported adsorbents for MG removal is summarized in Table 4. As shown, the BAC prepared in this study exhibits a higher q_{max} than several biochar-based materials derived from different biomass sources [1, 28, 29]. This observation suggests that chemical activation of biochar to activated

carbon is a crucial step in enhancing surface area and pore development, which in turn significantly improves the adsorption performance toward MG. However, the q_{max} of the prepared BAC is relatively lower than that reported for activated carbons derived from jackfruit peel and almond shell [30, 31]. This difference can be mainly attributed to the comparatively lower specific surface area and pore volume of BAC, as discussed in the BET analysis. Therefore, further enhancement of adsorption performance may be achieved through optimization of activation conditions, such as activating agent ratio and activation temperature, to promote pore development and increase surface area. In addition, post-activation surface modification by introducing appropriate functional groups (e.g., –COOH, $–SO_3H$, –OH, and $–NH_2$) has been reported to effectively enhance surface charge density and adsorption affinity toward cationic dyes [32, 33]. The combined optimization of activation conditions and surface functionalization is thus expected to further improve the adsorption capacity of BAC for MG removal.

Table 4. The maximum capacity of MG adsorbed by various adsorbents

Material	q_{max} (mg/g)	Reference
BAC	336.50	In this study
Algae biochar	1.98	[1]
Peanut shell biochar	202.18	[28]
Almond shell biochar	120.21	[29]
Jackfruit peel activated carbon	376.33	[30]
Almond shell activated carbon	363.60	[31]

IV. Conclusion

Bamboo-derived AC was successfully applied for the adsorption of MG from synthetic wastewater. Material characterization confirmed that BAC possesses favorable surface and textural properties for MG dye adsorption. Batch experiments showed rapid adsorption with equilibrium reached within 60 min, and isotherm analysis indicated that the Langmuir model best described the adsorption behavior. These findings suggest that BAC is an effective adsorbent for MG removal from aqueous systems.

Conflict of Interest

The authors declare no conflict of interest.

Author Contributions

Teewara Teerasukyodying and Nagone Luangphaiboonsri designed and conducted the experiments, analyzed the adsorption data of MG on BAC, and prepared the original manuscript. Weerawat Clowutimon and Pornsawan Assawasaengrat performed the material characterizations (SEM, CHNS, XRD, FT-IR, and BET) and revised the manuscript. All authors have read and approved the final version of the manuscript.

Acknowledgment

The equipment in this research was supported by Department of Chemical Engineering, Faculty of Engineering, Chulalongkorn University and Department of Chemical Engineering, School of Engineering, King Mongkut's Institute of Technology Ladkrabang.

References

[1] W. Z. Wu, R. Li, Z. Q. L. Ma, C. X. Liu, and W. T. Zhao, "Biochar-algae microspheres based on sodium alginate for the highly efficient adsorption of malachite green dye: Kinetics, isotherms, and mechanism of adsorption," *J. Contam. Hydrol,* vol. 272, 104547, March 2025.

[2] H. Yazid, T. Bouzid, A. Naboulsi, A. Grich, E. M. Mountassir, A. Regti, M. E. Himri, and M. E. Haddad, "Adsorption of malachite green using waste marine cuttlefish bone powder: Experimental and theoretical investigations," *Mar. Pollut. Bull.,* vol. 209, 117210, November 2024.

[3] Z. Wen, Y. Chen, F. Chen, X. Lan, P. Yang, Y. Ye, J. Lan, and L. Wu, "Ultra-high adsorption capacity of porous calcium carbonate for removal of malachite green from water," *Matter. Lett.,* vol. 396, 138763, May 2025.

[4] X. Cao, S. Sun, and R. Sun, "Application of biochar-based catalysts in biomass upgrading: A review," *RSC Adv.,* vol. 7, pp. 48793–48805, October 2017.

[5] T. W. Chew, P. S. H. Ng, B. C. T. G. L. C. Abdullah, K. L. Chin, C. L. Lee, B. M. S. M. N. Hafizuddin, and L. T. Mai, "A review of bio-based activated carbon properties produced from different activating chemicals during chemicals activation process on biomass and its potential for Malaysia," *Materials.* vol. 16, 7365, November 2023.

[6] Z. Heidarinejad, M. H. Dehghani, M. Heidari, G. Javedan, I. Ali, and M. Sillanpaa, "Methods for preparation and activation of activated carbon: A review," *Environ. Chem. Lett.,* vol. 18, pp. 393–415, January 2020.

[7] S. Kundu, T. Khandaker, M. A. M. Anik, M. K. Hasan, P. K. Dhar, S. K. Dutta, M. A. Latif, and M. C. Hossain, "A comprehensive review of enhance CO_2 capture using activated carbon derived from biomass feedstock," *RSC Adv.,* vol. 14, pp. 29693–29736, September 2024.

[8] H. Y. Wu, S. S. Chen, W. Liao *et al.*, "Assessment of agricultural waste-derived activated carbon in multiple applications," *Environ. Res.,* vol. 191, 110176, December 2020.

[9] S. F. Lo, S. Y. Wang, M. J. Tsai, and L. D. Lin, "Adsorption capacity and removal efficiency of heavy metal ions by Moso and Ma bamboo activated carbons," *ChERD*, vol. 9, pp. 1397–1406, September 2012.

[10] R. Thatagamuge, M. R. R. Kooh, A. H. Mahadi *et al.*, "Copper modified activated bamboo charcoal enhance adsorption of heavy metals from industrial wastewater," *Environ. Nanotechnol. Mon. Manage.,* vol. 16, 100562, December 2021.

[11] W. Wu, C. Wu, G. Zhang, J. Liu, Y. Li, and G. Li, "Synthesis and characterization of magnetic K_2CO_3-activated carbon produced from bamboo shoot for the adsorption of Rhodamine B and CO_2 capture," *Fuel,* vol. 332, 126107, September 2022.

[12] S. Wei, Z. Tan, Z. Liu, H, Zuo, Y. Xia, and Y. Zhang, "Removal of methyl orange dye by high surface area biomass activated carbon prepared from bamboo fibers," *Ind Crops Prod.,* vol. 218, 118991, June 2024.

[13] I. U. Bakara, M. D. Nurhafizah, N. Abullah, O.O. Akinowa, and A. Ul-Hamid, "Investigation of kinetics and thermodynamics of methylene blue dye adsorption using activated carbon derived from bamboo biomass," *Inorg. Chem. Commun.,* vol. 166, 112609, May 2024.

[14] R. Verma and M. Choudhary, "Optimization of chemical impregnation methods for the regeneration of spent activated carbon," *JCHR*, vol. 15, pp. 323–329, May 2025.

[15] T. A. M. Lima, M. S. T. Arantes, J. A. Araujo *et al.*, "Valorisation of invasive plant (*Phododendron ponticum*) biomass into activated biochar as a sustainable adsorbent for emerging pharmaceutical contaminant removal from water," *RSC Sustainable,* 2025. doi: 10.1039/d5su00589b

[16] C. Rekia, S. Derradji, O. Amira, C. Fatiha, C. Mounira, and B. Souhcyla, "Removal of Methylene blue using adsorption onto activated carbon derived from juniper berries," *Tob Regul Sci*., vol. 9, pp. 850–859, November 2023.

[17] D. Cuhadaroglu and O. A. Uygen, "Production and characterization of activated carbon from a bituminous coal by chemical activation," *Afr. J. Biotechnol.* vol. 7, pp. 3703–3710, October 2008.

[18] T. D. Hoang, Y. Liu, and M. T. Le, "Synthesis and characterization of biochar and activated carbons derived from various biomasses," *Sustain.,* vol. 16, 5495, June 2024.

[19] Y. Xu, D. Zhang, Y. Liu, Y. Xu, W. Meng, J. Zhong, R. Hu, and Z. Wu, "Elucidating the role of moderate K_2CO_3 activation in tuning microporous architecture of bamboo-derived activated carbon for superior CO_2 capture," *BMSBEO*, vol. 201, 108140, July 2025.

[20] W. Wu, C. Wu, J. Liu, H. Yan, G. Zhang, G. Li, Y. Zhao, and Y. Wang, "Nitrogen-doped porous carbon through K_2CO_3-activated bamboo shoot shell for an efficient CO_2 adsorption," *Fuel,* vol. 363, 130937, January 2024.

[21] S. Wei, Q. Qin, and Z. Liu, "Thermal behavior analysis and reaction mechanism in the preparation of activated by $ZnCl_2$ activation of bamboo fibers," *J. Anal. Appl. Pyrolysis,* vol. 179, 106500, April 2024.
[22] S. Muniandy, L. Salleh, and M. A. A. Zaini, "Evaluation of malachite green and methyl violet dues removal by 3A molecular sieve adsorbents," *Desalination Water Treat.,* vol. 203, pp. 440–448, November 2020.
[23] H. Marsh, and F. Rodriguez-Reinoso, *Activated Carbon*, 1st ed., Oxford, U.K.: Elsevier, 2006.
[24] M. A. Lillo-Rodenas, D. Cazorla-Amoros, and A. Linares-Salano, "Understanding chemical reactions between carbons and NaOH and KOH: An insight into the chemical activation mechanism," *Carbon*, vol. 41, pp. 267–275, Feb. 2003.
[25] K. Hall, L. C. Eagleton, A. Acrivos, and T. Vermeulen, "Pore and solid diffusion kinetics in fixed-bed adsorption under constant-pattern," *Ind. Eng. Che. Fund.*, vol. 5, pp. 212–223, Feb. 1966.
[26] A. S. Bhatt, P. L. Sakaria, M. Vasudevan, R. R. Pawar, N. Sudheesh, H. C. Bajaj, and H. M. Mody, "Adsorption of an anionic dye from aqueous medium by organoclays: Equilibrium modeling, kinetic and thermodynamic exploration," *RSC Adv.*, vol. 2, pp. 8663–8671, Oct. 2012.
[27] W. Qian, Y. Deng, Y. Zhang, Y. Li, Y. Fang, X. Li, J. Liang, and H. Liu, "Dyeing sludge-derived biochar for efficient removal of malachite green from dyeing wastewater," *WEC&N*, vol. 3, 18, Jul. 2024.
[28] J. Wang, H. Bai, W, Gao, J. Chen, M. Ren, D. Liu, Q. Zhang, and Z. Du, "Efficient adsorption of malachite green by layered double hydroxide loaded biochar: Characterization, performance, mechanisms and soil remediation," *J. Taiwan Inst. Chem. Eng.*, vol. 178, 106830, Sep 2025.
[29] F. Chouli, A. O. Ezzat, L. Sabantina, A. Benyoucef, and A. Zehhaf, "Optimization conditions of malachite green adsorption onto almond shell carbon waste using process design," *Molecules*, vol. 29, p. 54, Dec. 2023.
[30] M. F. M. Yusop, A. Z. Abdullah, and M. A. Ahmad, "Malachite green dye adsorption by jackfruit based activated carbon: Optimization, mass transfer simulation and surface area prediction," *DRM.*, vol. 136, 109991, Jun. 2023.
[31] A. Rial, C. H. Pimentel, D. Gomez-Diaz, M. S. Freire, and J. Gonzalez-Alvarez, "Evaluation of almond shell activated carbon for dye (methylene blue and malachite green) removal by experimental and simulation studies," *Materials*, vol. 17, p. 6077, Dec. 2024.
[32] K. Y. Foo and B. H. Hameed, "Insights into the modeling of adsorption isotherm systems," *Chem. Eng. J.*, vol. 156, pp. 2–10, Jan. 2010.
[33] S. Wang and Z. H. Zhu, "Effects of acidic treatment of activated carbons on dye adsorption," *Dyes Pigm.*, vol. 75, pp. 306–314, Jul. 2006.